19. Howard, J., Hudspeth, A. J. & Vale, R. D. Movement of microtubules by single kinesin molecules. *Nature* **342,** 154–158 (1989).
20. Hancock, W. O. & Howard, J. Processivity of the motor protein kinesin requires two heads. *J. Cell Biol.* **140,** 1395–1405 (1998).
21. Howard, J. & Hyman, A. A. Preparation of marked microtubules for the assay of the polarity of microtubule-based motors by fluorescence microscopy. *Methods Cell Biol.* **39,** 105–113 (1993).
22. Cole, D. G. *et al. Chlamydomonas* kinesin-II-dependent intraflagellar transport (IFT): IFT particles contain proteins required for ciliary assembly in *Caenorhabditis elegans* sensory neurons. *J. Cell Biol.* **141,** 993–1008 (1998).
23. Kojima, H., Muto, E., Higuchi, H. & Yanagida, T. Mechanics of single kinesin molecules measured by optical trapping nanometry. *Biophys. J.* **73,** 2012–2022 (1997).
24. Svoboda, K. & Block, S. M. Force and velocity measured for single kinesin molecules. *Cell* **77,** 773–784 (1994).
25. Paschal, B. M., Obar, R. A. & Vallee, R. B. Interaction of brain cytoplasmic dynein and MAP2 with a common sequence at the C terminus of tubulin. *Nature* **342,** 569–572 (1989).
26. King, S. M., Otter, T. & Witman, G. B. Purification and characterization of *Chlamydomonas* flagellar dyneins. *Methods Enzymol.* **134,** 291–306 (1986).
27. Vallee, R. B. Reversible assembly purification of microtubules without assembly-promoting agents and further purification of tubulin, microtubule-associated proteins, and MAP fragments. *Methods Enzymol.* **134,** 89–104 (1986).
28. Katayama, E. The effects of various nucleotides on the structure of actin-attached myosin subfragment-1 studied by quick-freeze deep-etch electron microscopy. *J. Biochem.* **106,** 751–770 (1989).
29. Jameson, D. M. & Eccleston, J. F. Fluorescent nucleotide analogs: Synthesis and applications. *Methods Enzymol.* **278,** 363–390 (1997).

Acknowledgements. We thank M. Anson for discussion and comments on the manuscript and M. Kikumoto for single molecule measurements. This work was partly supported by the Hyogo Science and Technology Foundation (K.O. and H.K.) and a grant-in-aid from the Ministry of Education, Science and Culture of Japan (K.O.).

Correspondence and requests for materials should be addressed to K.O. (e-mail: oiwa@crl.go.jp).

Myosin-V is a processive actin-based motor

Amit D. Mehta*, Ronald S. Rock*, Matthias Rief*, James A. Spudich*, Mark S. Mooseker† & Richard E. Cheney‡

* *Department of Biochemistry, Stanford University Medical Center, Stanford, California 94305, USA*
† *Department of Molecular, Cellular and Developmental Biology, Yale University, New Haven, Connecticut 06520, USA*
‡ *Department of Cell and Molecular Physiology, University of North Carolina at Chapel Hill, Chapel Hill, North Carolina 27599, USA*

Class-V myosins, one of 15 known classes of actin-based molecular motors, have been implicated in several forms of organelle transport[1–5], perhaps working with microtubule-based motors such as kinesin[2–4,6]. Such movements may require a motor with mechanochemical properties distinct from those of myosin-II, which operates in large ensembles to drive high-speed motility as in muscle contraction[7]. Based on its function and biochemistry, it has been suggested that myosin-V may be a processive motor[7,8] like kinesin[9,10]. Processivity means that the motor undergoes multiple catalytic cycles and coupled mechanical advances for each diffusional encounter with its track. This allows single motors to support movement of an organelle along its track. Here we provide direct evidence that myosin-V is indeed a processive actin-based motor that can move in large steps approximating the 36-nm pseudo-repeat of the actin filament.

Myosin-V purified from chick brain consists of two heavy chains, each with an amino-terminal head (motor) domain, a neck region supported by six light chains, a tail with a proximal coiled coil and a distal globular domain presumed to bind cargo and/or specify subcellular localization[1,11,12]. Myosin-V exhibits actin-activated ATP turnover and moves actin filaments *in vitro*[11]. To examine the dependence of movement on the number of motors, we measured this *in vitro* motility in 2 mM ATP for a wide range of myosin-V surface densities. At 54 molecules per μm^2 on the surface (600 pM added to flow chamber), myosin-V supported continuous and smooth actin-filament movement (287 ± 22 nm s^{-1}, $n = 60$). We continued to observe motility with myosin-V concentrations as low as 2.7 molecules per μm^2 (311 ± 70 nm s^{-1}, $n = 20$). At these very low surface densities of myosin-V, many actin filaments appeared to be tethered to the surface by a single contact point as they moved (Fig. 1a). Moreover, the moving filaments swivelled about the connection point, similar to behaviour reported for single kinesin molecule attachments[9]. Actin velocity did not fall as the myosin-V surface density was decreased from 1,000 to 2.7 molecules per μm^2 (data not shown).

To determine whether such motility is driven by single molecules or by coincident co-localization of several non-processive motors, we measured actin filament landing rates and distances moved over several decades of myosin-V surface density. We observed first-power dependence of the landing rate on surface density (Fig. 1b), as expected for a processive motor[9,13]. There was a gradual transition, from zero to one, in the fraction of filaments moving more than their length before releasing from the surface, as the myosin-V density on the surface was increased (Fig. 1c). The data (Fig. 1c) could be fitted to a functional form describing movement driven by a single molecule[9]: $1 - (\rho/\rho_o)\exp(-\rho/\rho_o)/(1 - \exp(\rho/\rho_o))$, where ρ is surface density and ρ_o is a fit parameter. These signatures of processivity[13], shared by kinesin[9,13] and myosin-V, differ markedly from those observed with single-headed kinesins[13], where four to six molecules are believed to be necessary and sufficient to propel sustained microtubule movement.

To examine single-molecule movement at high resolution, we used an optical trapping assay[14,15], with 10 pM myosin-V loaded in the flow cell (0.9 molecules per μm^2 on the surface). From system geometry, we estimate that we sample 0.09 μm^2 along the spherical platform surface, leading to an estimate of 0.08 accessible molecules per surface platform tested. As expected, we observed no binding events on ~90–95% of the surface platforms sampled. Were more than one molecule required for the behaviour observed, we would have detected no binding events in 99.7% of the platforms sampled[10]. In most binding events detected, the actin filament was bound and pulled for three-to-five step increments before dwelling at a stall point, detaching and returning to the baseline (Fig. 2a–c). Myosin-V stepped to a stall point, with stall force 3.0 ± 0.3 pN ($n = 25$) at 2 mM ATP, considerably less than the 5–8 pN observed for kinesin[16–19]. A lower stall force is expected for a motor with a larger step size (see below) if the maximum work output per step is similar for the two motors.

Load-dependent arrest of myosin-V movement may proceed through either or both of two mechanisms: first, load reduces the ATPase cycling rate by affecting a load-dependent biochemical transition (for example, release of the nucleotide hydrolysis product), as suggested for RNAP[20]; or, second, load affects the prob-

Table 1 Summary of step-size measurements

		Forward			Backward		
[ATP]	Frequency	*n*	Mean (nm)	s.d.	*n*	Mean (nm)	s.d.
2 mM	20 Hz	98	35.0	8.9	16	–36.3	8.5
2 mM	20 Hz	74	34.3	11.2	27	–37.0	13.2
2 mM	10 Hz	71	35.6	8.3	9	–38.8	9.2
2 mM	100 Hz	152	30.3	5.3	9	–27.5	11.8
10 μM	20 Hz	19	37.0	10.3	7	–29.0	10.2
1 μM	20 Hz	68	38.0	6.6	39	–36.0	9.1

All steps are measured for the left bead in Fig. 3a. Examples of forward events are as shown in Fig. 3b. Occasional backward events (not shown in Fig. 3) were seen in this experiment, similar to those seen in Fig. 2e.

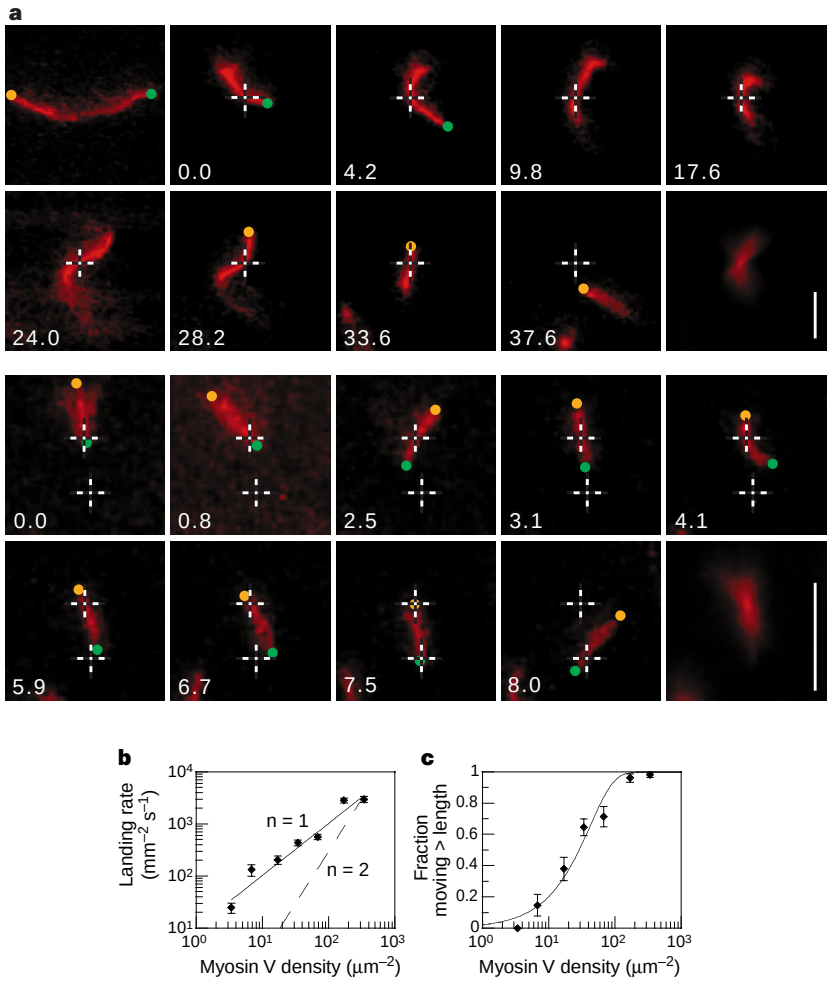

Figure 1 Actin-filament gliding. **a**, Actin filament moving over surface coated with 3.6 myosin-V molecules per μm^2 (2 mM ATP). The leading (green dots) and trailing (yellow dots) ends of the filament are marked when within the focal plane. Panels 1–10 (left right): time course (s) of a 16-μm actin filament before (panel 1) and after (panels 2–9) it bound to the surface. The filament remained connected at the in-focus contact point (crosshair), while the ends diffused in and out of the focal plane. Panel 10 shows the average image throughout the entire range of movement. Panels 11–20: movement (at 5.4 myosin-V molecules per μm^2) of a shorter filament whose diffusive motion was confined to the focal plane. The second crosshair points to a second attachment point. Scale: 5 μm. **b**, Actin-filament landing rates ($mm^{-2}\,s^{-1}$) as a function of surface myosin-V density. **c**, Fraction of filaments that moved more than their length before dissociating, as a function of surface density.

ability and direction of the mechanical step resulting from a catalytic cycle, as suggested for kinesin[16,17]. Our data favour a combination of the two for myosin-V. In support of the first proposal, as the load rises, dwell periods preceding forward steps become longer at 2 mM ATP but not at 1 μM ATP (Fig. 2d). This could mean, for example, that a load-decelerated ADP release no longer affects the ATPase cycling rate at 1 μM ATP, as ATP binding has become rate-limiting. Moreover, the load dependence of dwell periods at 2 mM ATP, rising sharply near stall, is consistent with those suggested to explain load-dependent chemistry (Fig. 2d)[20]. Consistent with the second mechanism, however, and as observed with kinesin[16–19], we frequently observed backward stepping at high load. Unlike anything observed with kinesin, we also observed sequences of two or three consecutive backward steps (Fig. 2e).

We performed optical trap experiments at 5 mM, 2 mM, 10 μM and 1 μM ATP. As the ATP concentration was dropped, dwell durations between steps at low load (where load and durations are uncorrelated) grew longer (0.08 ± 0.01 ($n = 37$), 0.10 ± 0.02 ($n = 64$), 0.28 ± 0.08 ($n = 12$) and 1.56 ± 0.12 ($n = 212$) s, respectively). Dwell-period durations at 1 μM ATP obey single-exponential statistics, indicating[19,21,22] that one ATP is coupled to one mechanical advance. Multiplying the dwell times by gliding velocities (54 molecules per μm^2, $n = 60$ at each ATP) at these four ATP concentrations yields 22–30 nm, 23–35 nm, 20–36 nm and 21–35 nm, respectively (range from propagated uncertainty). These remarkably consistent numbers overlap substantially the range of direct step measurements, to which we now turn.

The step sizes observed in the standard optical trap assay (Fig. 2a–c) are limited by compliance in the various connections (bead to actin filament and myosin-V to surface), and perhaps in the molecule itself[23]. These compliances cause the advance in bead position to reflect only part of myosin-V's advance along the actin filament. To circumvent compliance issues, we placed large-amplitude sinusoidal or triangle wave oscillations on one of the two trapped beads (Fig. 3a, left bead). When the bead in the oscillated trap was pulled by myosin-V from its trap centre, we observed clipping in the bead oscillation, presumably because the system, including the myosin-V molecule and its surface attachment, was pulled taut. By examining the clipped level, we measured the tether length between the trapped bead and the myosin-V molecule, which decreased in increments as myosin-V stepped along the actin filament (Fig. 3a, b). Six different data sets each gave a broadly distributed step-value distribution, five centred about 34–38 nm and one about 30 nm (Fig. 3c, Table 1).

A step size of 30–38 nm (exceeding the 4–17-nm range of myosin-II step estimates[24] and the 8-nm kinesin step estimate[25]) is

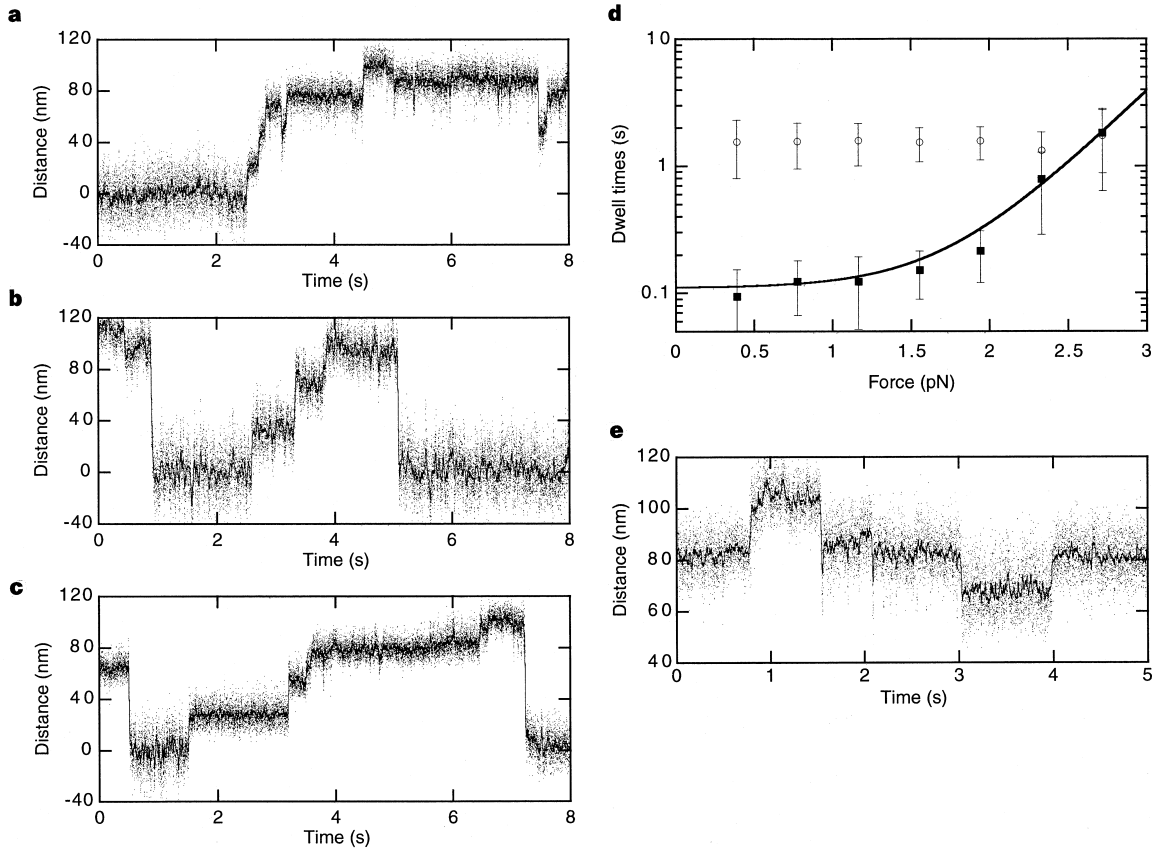

Figure 2 Processive stepping by myosin-V observed using the dual-beam optical trap. **a**–**c**, Sample traces of stepping behaviour at 2 mM, 10 μm and 1 μM ATP, respectively. Dwell periods T_i at 1 μM ATP fit single exponential statistics, as judged by (mean$\{T_i|T_i > \tau_o\} - \tau_o$) remaining constant against varying τ_o (ref. 30). **d**, Mean dwell time as a function of load, at 2 mM ATP (squares) and at 1 μM ATP (circles). **e**, Backward stepping behaviour (at 1.5 s and 3 s) at high load in 1 μM ATP.

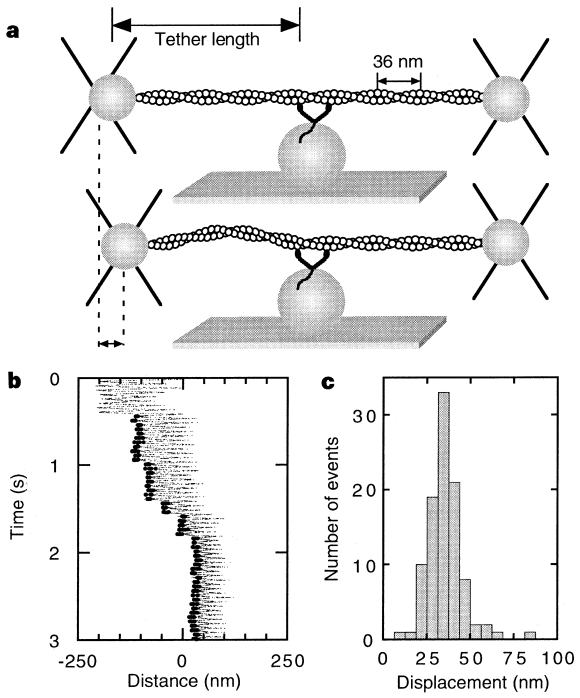

Figure 3 Step measurements. **a**, The scheme of the oscillation experiments (see Methods). **b**, Sample trace at 2 mM ATP. The myosin molecule bound the actin just before the 0.5-s mark. After this, the bead ceased to follow the driving triangle wave for a fraction of each oscillation. **c**, Sample histogram of step increments so measured.

plausible given that ~100° angle between two ~23 nm necks can subtend this distance[7]. Interestingly, this step size may allow the molecule to step along the 36-nm pseudo-repeat of the actin helix. This would allow a single myosin-V molecule and its cargo to move along a single filament without spiralling around it. However, the spread in the step-size measurements (Table 1) exceeds the <~4-nm measurement precision. This spread raises the possibility that myosin-V may not move precisely along the pseudo-repeat, but rather can bind along the filament at different points while still approximating the pseudo-repeat on average. Alternatively, a randomizing effect in the assay[26] (for example, limited actin rotation, shifting randomly the next myosin binding site on the actin filament) may underlie the distribution width.

These data allow us to estimate the average minimum number of steps a single myosin-V molecule can make at zero load before releasing the actin for long enough to diffuse away. We estimate a minimum mean Λ of travel lengths L_i of 1.6 μm ($n = 27$) (measured from surface attachment to release in Fig. 1 assays, 2 mM ATP, 3.5 molecules per μm^2, with nodal swivelling). We compute this using (mean$\{L_i|L_i > L_t\} - L_t$), thus assuming that it is exponentially distributed[10] with a low-end reliable measurement threshold $t_i = 2$ μm. As many filaments were moved by myosin-V to their ends and released only then, Λ is certainly an underestimate. From this we estimate that myosin-V can take at least 40–50 steps on average before releasing actin.

Although class-V myosins are related in sequence and structure to muscle myosin-II, they face a significantly different biological task: movement of cargo by relatively few motors in regions containing relatively few actin filaments. A processive motor could more easily perform the roles suggested by myosin-V-dependent endoplasmic

reticulum vesicle transport[2], messenger RNA transport in yeast[27] and organelle transport generally[1,3–5]. Moreover, prolonged contact between myosin-V and its actin track may underlie its proposed role as an organelle tether. Such a role has been indicated by myosin-V-dependent retention of smooth endoplasmic reticulum with dendritic spines of Purkinje neurons[4] and retention of melanosomes within the dendrites of melanocytes[1,3]. The findings reported here, using single-molecule analysis, fit well with the expected roles of class-V myosins and demonstrate the existence of processivity within the myosin superfamily. □

Methods

Gliding filament assay. In all assays described, motility buffers[15] (23 °C) included 25 mM imidazole HCl, pH 7.4, 25 mM KCl, 1 mM EGTA, 10 mM DTT, with variable Mg–ATP, an ATP-regenerating system (1 mM phosphocreatine, 0.1 mg ml^{-1} creatine phosphokinase) and an oxygen-scavenging system to retard photobleaching (25 μg ml^{-1} glucose oxidase, 45 μg ml^{-1} catalase and 1% glucose). Myosin-V was purified as described[28]. To quantify filament-landing rates (Fig. 1b), we scored as 'landed' a filament that had touched down and moved for >0.5 μm over 2 s. Landing assays were performed at 2 mM ATP with constant actin concentration (5 μg ml^{-1}). All surface myosin-V densities given assume that every molecule entered the flow cell, none suffered damage, and half adsorbed to each surface of the flow cell. Electron microscopy (EM) analysis[11] and atomic-force microscopy imaging in solution (not shown) indicated that myosin-V molecules adsorbed at 100 nM to a surface do not oligomerize, and analytical ultracentrifugation in the storage buffer showed a single well-defined boundary with an *s* value of 12.52 (O. C. Rodriguez and R. E. Cheney, personal communication). We observed the same actin landing rates at 6.8 myosin-V molecules per μm^2 after storage, dilution and adsorption of myosin-V in the motility assay buffer[15], myosin-V storage buffer[28] or the buffer used in the EM experiments[11]. Kinetic arguments exclude aggregation of protein on the surface[9]. Working at low densities required pre-adsorbing 10 μg ml^{-1} BSA on the surface (2 min incubation), before the addition of myosin. Similar pre-adsorption was necessary to observe motility under very low densities of kinesin[9,10]. To measure filament speed, we recorded and digitized visual fields at 30 frames s^{-1} and identified filament end positions. At low density, when the filament ends diffused into the image focal plane, we measured the contour length separating the fixed contact point to the filament end. As position (over 2–4 μm in 5–30 s) advances in time with constant position-detection error (0.2 μm), we can determine velocities reliably by measuring over sufficient length intervals. The error bars in Fig. 1b, c, are standard errors derived from counting statistics[13]. Velocity measurements are reported with standard deviations.

Optical trap. A single actin filament attached at both ends to optically trapped 1-μm-diameter polystyrene beads was stretched to tension and moved near to surface-bound silica spheres, decorated sparsely with myosin-V molecules. Both polystyrene beads were tracked with nanometre and millisecond resolution[15]. We used a biotin–avidin system to link actin to the polystyrene beads[29].

Load-dependent dwell times. To compute the load burdening a molecule, we summed the forces exerted on the molecule by each of the two traps (16 and 30 fN nm^{-1}). We measured the duration of dwell periods separating step transitions and preceding forward-directed ones. Uncertainties in these and other dwell times are computed as described[30]. Assuming load-dependent chemistry at 2 mM ATP, we fitted the data with $\tau = \tau 1 + \tau 2 \exp(F\delta/k_BT)$[20], where τ is the dwell time, $\tau 1$ represents load-independent transitions, $\tau 2$ load-dependent transitions, F the load, δ the 'characteristic distance' over which load affects stall (not necessarily the step size) and k_BT the thermal energy, to generate the solid curve shown in Fig. 2d. We extracted the following best-fit parameters: $\tau 1/\tau 2 > 100$, indicating that load-independent biochemical transitions are >100-fold slower than mechanical ones at vanishing load; and δ ranges from 10 to 15 nm, on the order of but less than the measured step size. These conclusions are unaffected by changes in binning parameters.

Step-size measurements (see Fig. 3). A 270-nm peak-to-peak triangle wave (double arrow separating dashed lines in Fig. 3a) was applied to the optical trap on the left (stiffness 16 fN nm^{-1}), moving the actin filament between a taut state and a compliant state. As myosin binds and pulls the filament to the right, the total trapped bead-to-surface platform linkage oscillates between states of very high and very low tension. To measure step sizes we monitored the mean position of the clipped (artificially darkened in Fig. 3b) part in each oscillation cycle as the bead continued to step. We measured steps (in nm) with oscillations at 10, 20 and 100 Hz at 2 mM ATP, and 20 Hz at 10 μM and 1 μM ATP (Table 1). Step amplitudes were only weakly correlated with displacement from baseline, indicating that all compliance had been similarly removed throughout the range of stepping. We scored only transitions with more than three cycles of dwell at a consistent position on both starting and ending level. Outliers may reflect the occasional incidence of two steps within one oscillation cycle. □

Received 23 March; accepted 23 June 1999.

1. Wu, X., Bowers, B., Rao, K., Wei, Q. & Hammer, J. A. Visualization of melanosome dynamics within wild-type and dilute melanocytes suggests a paradigm for myosin-V function *in vivo*. *J. Cell Biol.* **143,** 1899–1918 (1998).
2. Tabb, J. S., Molyneaux, B. J., Cohen, D. L., Kuznetsov, S. A. & Langford, G. M. Transport of ER vesicles on actin filaments in neurons by myosin-V. *J. Cell Sci.* **111,** 3221–3234 (1998).
3. Rogers, S. L. & Gelfand, V. I. Myosin cooperates with microtubule motors during organelle transport in melanophores. *Curr. Biol.* **8,** 161–164 (1998).
4. Mermall, V., Post, P. L. & Mooseker, M. S. Unconventional myosins in cell movement, membrane traffic and signal transduction. *Science* **279,** 527–533 (1998).
5. Evans, L. L., Lee, A. J., Bridgman, P. C. & Mooseker, M. S. Vesicle-associated brain myosin-V can be activated to catalyze actin-based transport. *J. Cell Sci.* **111,** 2055–2066 (1998).
6. Huang, J. D. *et al.* Direct interaction of microtubule- and actin-based transport motors. *Nature* **397,** 267–270 (1999).
7. Howard, J. Molecular motors: structural adaptations to cellular functions. *Nature* **389,** 561–567 (1997).
8. Nascimento, A. A. C., Cheney, R. E., Tauhata, S. B. F., Larson, R. E. & Mooseker, M. S. Enzymatic characterization and functional domain mapping of brain myosin-V. *J. Biol. Chem.* **271,** 17561–17569 (1996).
9. Howard, J., Hudspeth, A. J. & Vale, R. D. Movement of microtubules by single kinesin molecules. *Nature* **342,** 154–158 (1989).
10. Block, S. M., Goldstein, L. S. & Schnapp, B. J. Bead movement by single kinesin molecules studied with optical tweezers. *Nature* **348,** 348–352 (1990).
11. Cheney, R. E. *et al.* Brain myosin-V is a two-headed unconventional myosin with motor activity. *Cell* **75,** 13–23 (1993).
12. Reck-Peterson, S. L., Novick, P. J. & Mooseker, M. S. The tail of a yeast class V myosin, myo2p, functions as a localization domain. *Mol. Biol. Cell* **10,** 1001–1017 (1999).
13. Hancock, W. O. & Howard, J. Processivity of the motor protein kinesin requires two heads. *J. Cell Biol.* **140,** 1395–1405 (1998).
14. Finer, J. T., Simmons, R. M. & Spudich, J. A. Single myosin molecule mechanics: piconewton forces and nanometre steps. *Nature* **368,** 113–119 (1994).
15. Mehta, A. D., Finer, J. T. & Spudich, J. A. Use of optical traps in single-molecule study of nonprocessive biological motors. *Methods Enzymol.* **298,** 436–459 (1998).
16. Svoboda, K. & Block, S. M. Force and velocity measured for single kinesin molecules. *Cell* **77,** 773–784 (1994).
17. Meyhofer, E. & Howard, J. The force generated by a single kinesin molecule against an elastic load. *Proc. Natl Acad. Sci. USA* **92,** 574–578 (1995).
18. Coppin, C. M., Pierce, D. W., Hsu, L. & Vale, R. D. The load dependence of kinesin's mechanical cycle. *Proc. Natl Acad. Sci. USA* **94,** 8539–8544 (1997).
19. Kojima, H., Muto, E., Higuchi, H. & Yanagida, T. Mechanics of single kinesin molecules measured by optical trapping nanometry. *Biophys. J.* **73,** 2012–2022 (1997).
20. Wang, M. D. *et al.* Force and velocity measured for single molecules of RNA polymerase. *Science* **282,** 902–907 (1998).
21. Schnitzer, M. J. & Block, S. M. Kinesin hydrolyses one ATP per 8-nm step. *Nature* **388,** 386–390 (1997).
22. Hua, W., Young, E. C., Fleming, M. L. & Gelles, J. Coupling of kinesin steps to ATP hydrolysis. *Nature* **388,** 390–393 (1997).
23. Howard, J. & Spudich, J. A. Is the lever arm of myosin a molecular elastic element? *Proc. Natl Acad. Sci. USA* **93,** 4462–4464 (1996).
24. Mehta, A. D. & Spudich, J. A. Single myosin molecule mechanics. *Adv. Struct. Biol.* **5,** 229–270 (1999).
25. Svoboda, K., Schmidt, C. F., Schnapp, B. J. & Block, S. M. Direct observation of kinesin stepping by optical trapping interferometry. *Nature* **365,** 721–727 (1993).
26. Molloy, J. E., Burns, J. E., Kendrick-Jones, J., Tregear, R. T. & White, D. C. Movement and force produced by a single myosin head. *Nature* **378,** 209–212 (1995).
27. Bertrand, E. *et al.* Localization of ASH1 mRNA particles in living yeast. *Mol. Cell* **2,** 437–445 (1998).
28. Cheney, R. E. Purification and assay of myosin-V. *Methods Enzymol.* **298,** 3–18 (1998).
29. Ishijima, A. *et al.* Simultaneous observation of individual ATPase and mechanical events by a single myosin molecule during interaction with actin. *Cell* **92,** 161–171 (1998).
30. Veigel, C. *et al.* The motor protein myosin-I produces its working stroke in two steps. *Nature* **398,** 530–533 (1999).

Acknowledgements. We thank O. Rodriguez, C. Pennisi and C. Pearson for assistance in the purification of myosin-V; T. Sulchek for assistance in AFM imaging; J. Sellers for helpful discussions; and L. Evans, V. Mermall, H. Warrick, and M. Heidecker for their comments on the manuscript.

Correspondence and requests for materials should be addressed to A.D.M. or R.E.C.